

# Supplemental Information

## Biobased Superhydrophobic Coating Enabled by Nanoparticle Assembly

Emily Olson<sup>1,2</sup>, Jonathan Blisko<sup>3</sup>, Chuanshen Du<sup>1</sup>, Yi Liu<sup>4</sup>, Yifan Li<sup>1</sup>, Henry Thurber<sup>1,2</sup>, Greg Curtzwiler<sup>2,5</sup>, Juan Ren<sup>4</sup>, Martin Thuo<sup>1</sup>, Xin Yong<sup>3</sup>, Shan Jiang<sup>1,2\*</sup>

<sup>1</sup>Department of Materials Science and Engineering, Iowa State University, Ames IA 50011

<sup>2</sup>Polymer and Food Protection Consortium, Iowa State University, Ames IA 50011

<sup>3</sup>Department of Mechanical Engineering, Binghamton University, Binghamton NY 13902

<sup>4</sup>Department of Mechanical Engineering, Iowa State University, Ames IA 50011

<sup>5</sup>Department of Food Science and Human Nutrition, Iowa State University, Ames IA 50011

\*Corresponding author, to whom all correspondence is addressed. Email: [sjiang1@iastate.edu](mailto:sjiang1@iastate.edu)

Keywords: Biobased, coating, nanoparticle, self-assembly, superhydrophobic

## Scaling of AFM Force Data

*In-situ* liquid-phase AFM measurement provides the force between the microscale colloidal probe and the flat substrate within the polymer solution. However, Langevin dynamics simulation requires an effective interaction potential between two particles representing silica nanoparticles of size 100 nm, given in an analytic functional form. To obtain a usable interparticle potential for simulation, the force data obtained from AFM (**Figure 1a**) must be properly scaled to account for the geometric difference of the interacting surfaces. We employ the Derjaguin approximation<sup>1</sup> for the force scaling. This approach divides the surfaces of the two interacting bodies into concentric rings. A dimensionless scaling parameter is introduced when the surface interaction is obtained through the integration over the discretized surfaces. For two isotropically curved surfaces, the scaling parameter simplifies to

$$R' \equiv R_1 R_2 / (R_1 + R_2)$$

where  $R_1$  and  $R_2$  are the radii of curvature of the two surfaces. In the AFM measurement, we consider  $R_1 = R_{probe}$  and  $R_2 = \infty$  for the probe and flat substrate respectively, which give  $R'_{AFM} = R_{probe}$ . For the interaction between two nanoparticles,  $R_1 = R_2 = \sigma/2$  with  $\sigma$  being the particle diameter and thus  $R'_{pp} = \sigma/4$ . Using experimental values of  $\sigma = 100$  nm and  $R_{probe} = 2.5$   $\mu\text{m}$ , the effective force between particles  $F_{pp}$  can be scaled as  $F_{pp} = (R'_{pp}/R'_{AFM})F_{AFM}$ , with  $F_{AFM}$  being the original AFM force data.

The resulting interparticle force curves are numerically integrated using the trapezoidal method to obtain the potential  $U = -\int F dr$ . The AFM-derived potential profiles (**Figure S3**) were then fitted using simple polynomial regression, the result of which is seen in **Figure 1b**. For the HES system, the fitting was achieved using a single 4<sup>th</sup> degree polynomial, given by

$$U_{HES}(r/\sigma) = 24.85 - 77.92(r/\sigma) + 77.62(r/\sigma)^2 - 31.78(r/\sigma)^3 + 4.663(r/\sigma)^4.$$

The range of interaction is  $0 \sigma \leq r \leq 2.25 \sigma$ . However, the HEC system requires a piecewise fit due to its steep onset of strong attraction. The short-range interaction is given by

$$U_{HEC}(r/\sigma) = 6.778 - 26.26(r/\sigma) + 9.342(r/\sigma)^2 + 2.555(r/\sigma)^3$$

for  $0 \sigma \leq r \leq 1.58 \sigma$ , while the long-range interaction is rather linear with a functional form  $U_{HEC}(r/\sigma) = -2.530 + 0.8094(r/\sigma)$  for  $1.58 \sigma \leq r \leq 3.17 \sigma$ . Both potentials exhibit long-range attraction and short-range repulsion. It is noteworthy that the repulsion remains finite at zero interparticle distance, which represents a soft-core particle. This interaction potential is reminiscent of the ones used in dissipative particle dynamics<sup>2</sup>. As discussed below, because particles are highly prone to aggregation at short distances, the soft-core repulsion does not have notable influence on particle dynamics and assembly structure evolution.

## Simulation Method

We simulate the assembly of silica nanoparticles in HEC and HES solutions using coarse-grained Langevin dynamics. Each nanoparticle is modeled as a coarse-grained Brownian particle and the polymer solution is implicitly modeled as the background medium. The dynamics of individual nanoparticles are governed by the Langevin equation  $m\ddot{\mathbf{r}}_i = -\frac{\partial U_i}{\partial \mathbf{r}_i} - \zeta\dot{\mathbf{r}}_i + \mathbf{g}_i(t)$ , where  $m$  is the mass of the particle,  $\zeta$  is the friction coefficient, and  $\mathbf{g}_i(t)$  is Gaussian white noise. The magnitudes of the frictional force and the thermal fluctuations are related through the fluctuation-dissipation theorem, so that the temperature of the system is maintained. The potential energy of the  $i$ th particle is calculated based on the summation of pairwise interparticle potentials from all neighbors within

a cutoff radius  $r_c$  as  $U_i(\mathbf{r}_i) = \sum_{j \neq i} U_{ij}(r_{ij})$ . The pairwise interaction represents the effective interaction between nanoparticles dispersed in the polymer solution. In contrast to previous studies using theoretical potentials<sup>3,4</sup>, we develop an interparticle potential based on the liquid-phase AFM measurement of adhesion forces between silica surfaces in HEC and HES solutions.

We consider nanoparticles reversibly assemble into clusters, which then move as rigid bodies. The rigid body dynamics of the clusters are also governed by the Langevin equations with both translational and rotational diffusion incorporated. We designate each particle as either free (type 1) or clustered (type 2) in order to track the evolution of particle clusters and separate the dynamics of isolated particles and clusters. The recognition of particle clusters is conducted based on the particle type and interparticle distance. Inspired by Gervasio and Lu's work<sup>4</sup>, the reversible assembly is implemented through a Monte Carlo scheme. Every Monte Carlo step is composed of aggregation and separation events. An aggregation event is defined for a pair of nanoparticles that interact with each other. According to the instantaneous interaction potential of the particle pair, a Metropolis criterion is applied to determine whether the aggregation succeeds or not. Namely, the probability of particle aggregation is calculated as  $P_a = 1 - \min(1, e^{U_{ij}/k_B T})$ , meaning that aggregation occurs only when the energy of attraction of the particle pair is sufficiently large to overcome thermal fluctuations. The pairwise event not only enables the initiation of clusters from isolated free particles and the growth of existing clusters via addition of free particles, but also readily captures the cluster-cluster aggregation. If an aggregation event is accepted, we assume that particles and clusters collide inelastically with their translational and angular momenta conserved<sup>4</sup>. The particles participating in aggregate events changes to type 2.

In contrast to the pairwise aggregation, the separation event is applied to individual particles in the existing clusters (type 2) using a different Metropolis criterion. The separation of particle  $i$  is

dictated by its total energy of interaction with its neighbors in the same cluster that are within the cutoff radius. The probability of success is given by  $P_s = \min(1, e^{E_i/k_B T})$  with  $E_i = \sum_{j \in C_n} U_{ij}$ , where  $C_n$  represents the cluster of index  $n$  that contains particle  $i$ . The particles separated from the clusters are designated as free particles (type 1) again and their dynamics no longer follow the rigid body motion of the clusters. Notably, the separation of one large cluster into multiple small clusters can be indirectly captured with the single-particle-based separation event with the help of cluster recognition. It is critical to incorporate the separation event so that nanoparticle aggregates can relax under thermal fluctuations.

All distances within the simulation are presented in terms of the particle diameter  $\sigma$ . The characteristic energy scale is selected to be the thermal energy  $k_B T$  at room temperature, where  $k_B$  is Boltzmann's constant. A characteristic time scale can be defined as  $\tau = \sigma \sqrt{m/k_B T}$ . For simplicity, the simulation results are presented in reduced units with  $\sigma$ ,  $k_B T$ ,  $m$ , and  $\tau$  all set to 1. To create an accurate comparison between the simulation and experiment, the approximate number of particles as were in the experimental solution were randomly dispersed throughout the simulation box. This was performed in a cubic domain for three different concentrations, 0.16 wt%, 0.8 wt%, and 3.0 wt%, with a box side length of 200, 150, and 100, respectively. The corresponding numbers of particles are 9,224, 19,460, and 21,621 for the respective concentrations. To enable proper tracking of cluster formation, the simulation domain is non-periodic and repulsive walls are placed at all six boundaries to prevent particles from leaving. The equation of motion is integrated using velocity-Verlet algorithm with the single-particle friction coefficient set to 0.1 to ensure small temperature fluctuations. Each simulation typically runs for 1 million time steps with a time step of 0.005. The simulation is performed using LAMMPS<sup>6</sup> with in-house modifications.

## References

- [1] Derjaguin, B. Untersuchungen über die Reibung und Adhäsion, IV. *Kolloid-Zeitschrift* **69**, 155–164 (1934)
- [2] Groot, R.D.; Warren, P.B. *J. Chem. Phys.* **107**, 4423-4435 (1997)
- [3] Snowden, M.J.; Clegg, S.M.; Williams, P.A.; Robb, I.D. *J. Chem. Soc. Faraday Trans.* **87**, 2201-2207 (1991)
- [4] Gervasio, M.; Lu, K. *Langmuir* **35**, 161-170 (2019)
- [5] Jungblut, S.; Joswig, J.-O.; Eychmüller, A. *Phys. Chem. Chem. Phys.* **21**, 5723-5729 (2019)
- [6] Plimpton, S. *J. Comp. Phys.* **117**, 1-19 (1995)

## Supplemental Figures

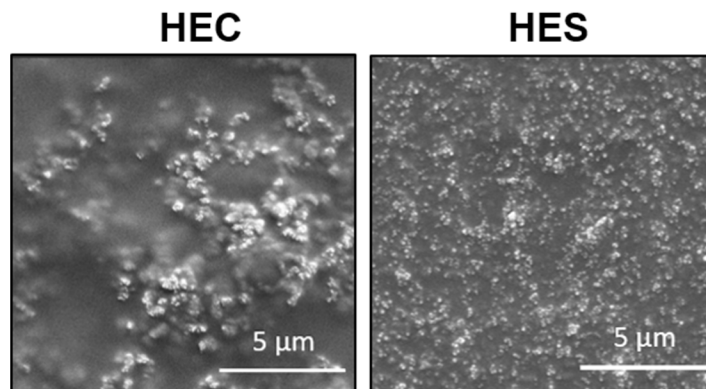


**Figure S1.** 0.16% wt. 100 nm silica in dried HEC and HES polymer coatings via SEM.

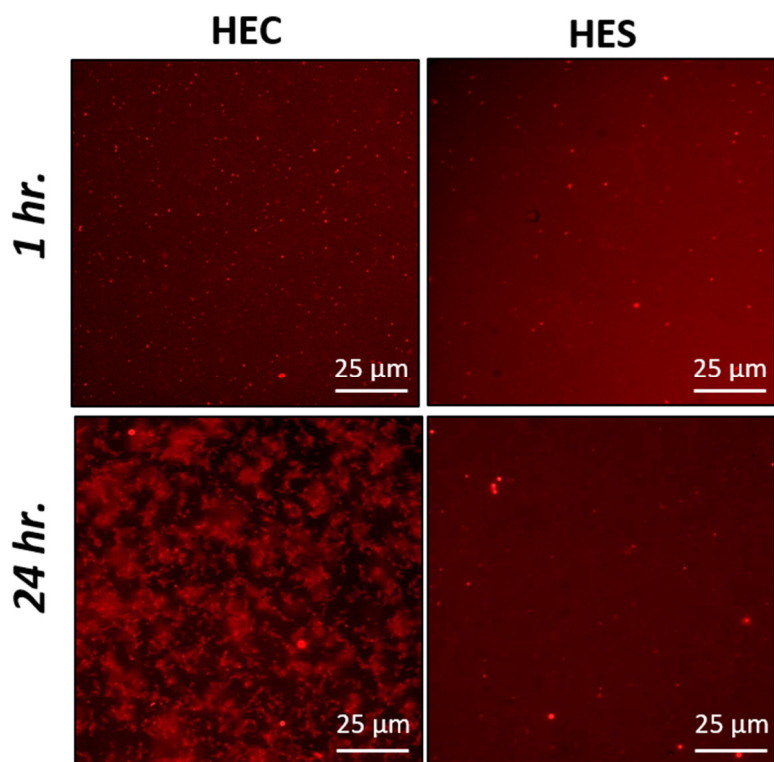


**Figure S2.** Fluorescent microscopy time lapse of the assembly of 0.16 wt. % silica nanoparticles in HEC and HES aqueous solutions.

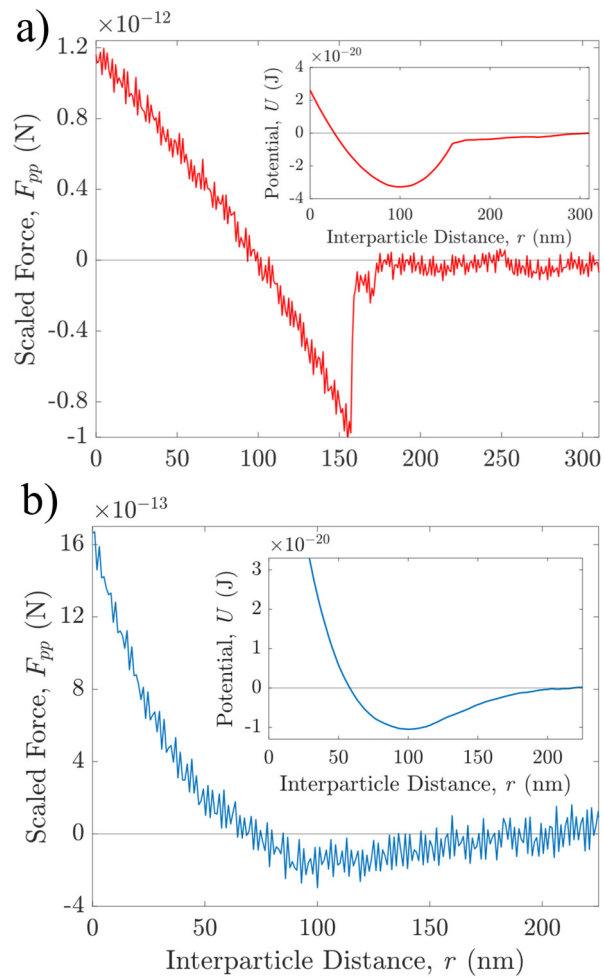


**Figure S3.** Scaled interaction forces between a pair of 100-nm nanoparticles dispersed in a) HEC; b) HES solutions. The insets are the corresponding potential profiles obtained by the numerical integration.



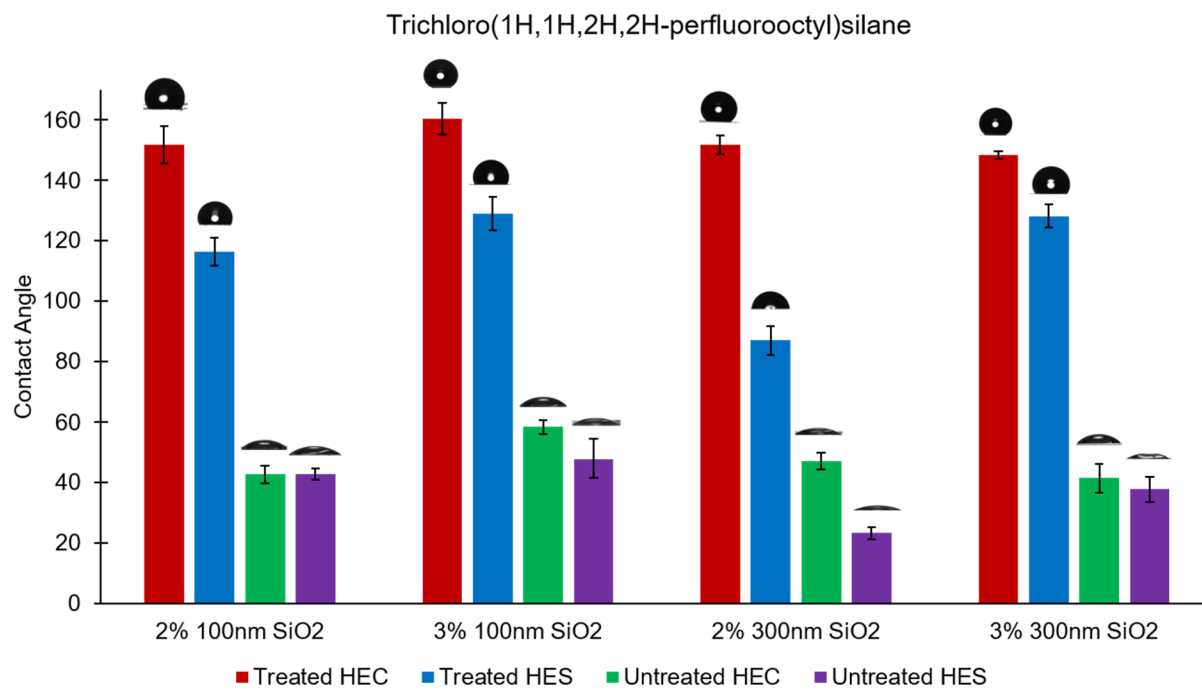


**Figure S4.** Contact angle of untreated (control) and trichloro(1H,1H,2H,2H-perfluorooctyl) silane treated sample films.

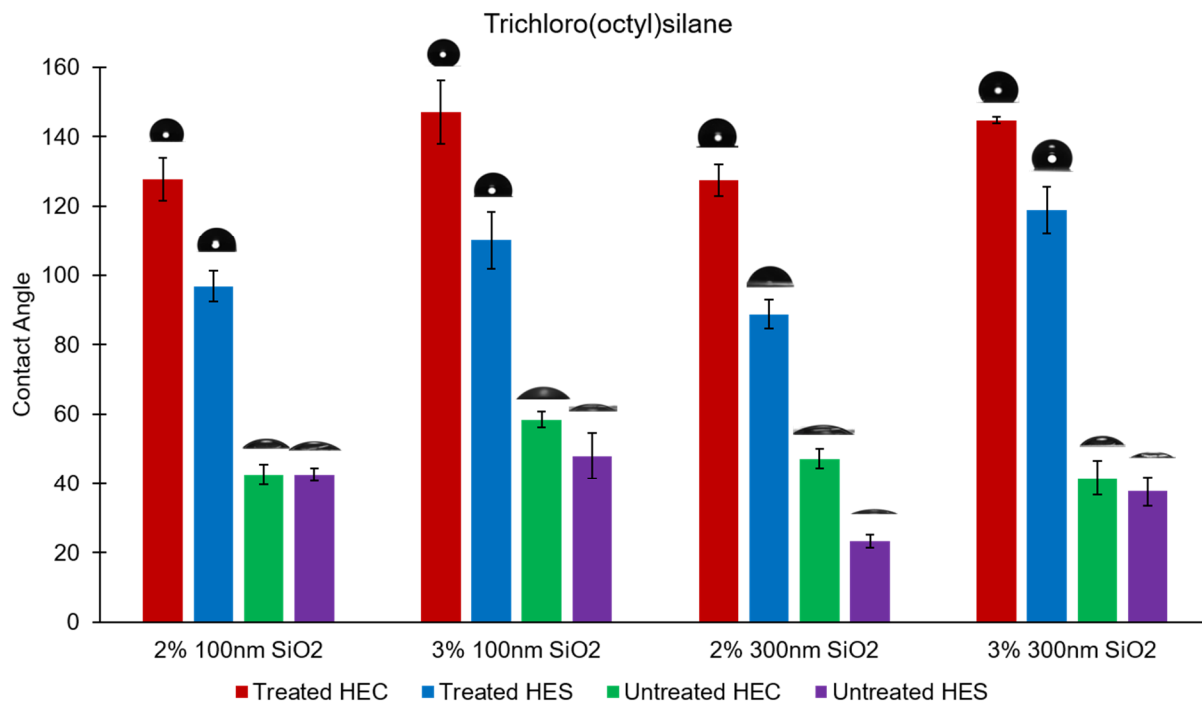


**Figure S5.** Contact angle of untreated (control) and trichloro(octyl) silane treated sample films.

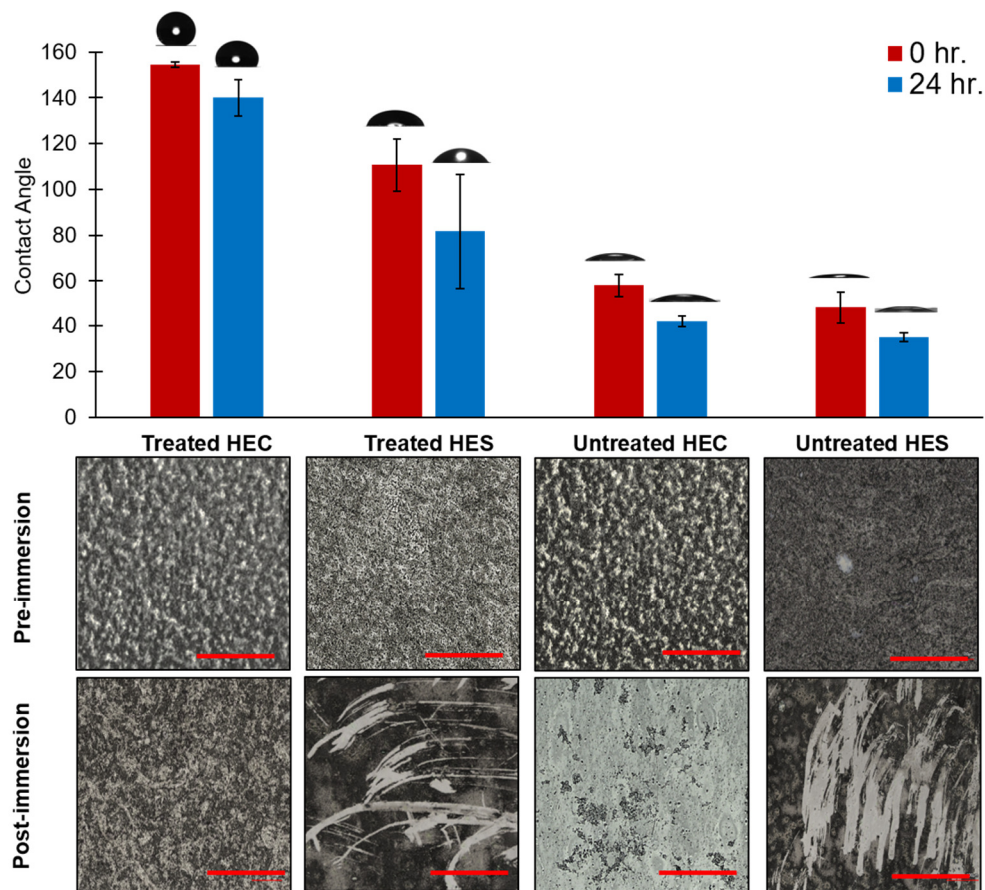


**Figure S6.** Contact angle measurements and corresponding confocal optical images: trichloro(octyl) silane treated samples with 3% 100 nm silica post immersion in water for 24 hours. Scale bar is 200  $\mu\text{m}$ .